1.0

2.8 | 2.5
3.2 | 2.2
3.6

2.0

1.1

1.8

1.25 | 1.4 | 1.6

MICROCOPY RESOLUTION TEST CHART
NATIONAL BUREAU OF STANDARDS

LEVEL 1

IRREVERSIBILITY AND TRANSPORT IN THE

LOWER HYBRID DRIFT INSTABILITY

by

J. F. Drake

March 1980

DTIC
ELECTE
AUG 12 1980
S
C

UNIVERSITY OF MARYLAND
DEPARTMENT OF PHYSICS AND ASTRONOMY
COLLEGE PARK, MARYLAND

80 6 20 161

IRREVERSIBILITY AND TRANSPORT IN THE
LOWER HYBRID DRIFT INSTABILITY.

J. F. Drake
Department of Physics and Astronomy,
University of Maryland,
College Park, Maryland 20740
N00014-79-C-0665

ABSTRACT

The dynamics of electrons in a low-frequency wave propagating perpendicular to a uniform magnetic field are studied and the implications of these results for transport and heating by the lower hybrid drift instability are explored. Below a threshold $e\phi/T_i \approx$ .25-.5, all electron energy and momentum exchange with the wave are reversible and no plasma transport is possible. Above this threshold, trapping of electrons by the wave potentials takes place and causes irreversible electron heating and momentum exchange. These results imply that anomolous transport in inhomogeneous plasma with weak drifts (diamagnetic velocity less than the ion thermal velocity) may be substantially less than previously predicted.

1. INTRODUCTION

The subject of heating and transport in high-temperature, magnetically-confined plasma, where classical collisional processes are weak, is of great importance both in achieving thermonuclear fusion in laboratory confinement systems and in understanding fundamental natural phenomena such as magnetic substorms. Instabilities whose source of free energy is the plasma density or magnetic field gradients are likely to produce fluctuating electric or magnetic fields which cause crossfield particle transport. In systems with rather sharp density gradients where $\rho_i/L_n > (m_e/m_i)^{1/2}$, ρ_i and L_n being the ion Larmor radius and density scale length, respectively, the lower-hybrid-drift instability is unstable and is expected to play a dominant role in the evolution of the plasma profiles.[1-5] Such sharp gradients occur in a variety of physical systems including laboratory plasmas such as θ-pinches and reversed-field pinches and space plasmas in the bow and tail of the earth's magnetosphere. The linear properties of this mode have been extensively investigated.[1-3] The instability is driven by the pressure gradient and is characterized by a frequency ω and growth rate γ given by $\omega \sim kv_{di}$ $\sim (\rho_i/L_n)\omega_{1h} \gg \Omega_i$, $\gamma \stackrel{<}{\sim} \omega$, where v_{di} is the ion diamagnetic velocity, Ω_i is the ion gyrofrequency and ω_{1h} is the lower hybrid frequency. The growth rate of the instability is sharply peaked perpendicular to $\underset{\sim}{B}$ ($k_{\parallel} = \underset{\sim}{k} \cdot \hat{\underset{\sim}{B}} \stackrel{\sim}{\sim} 0$) since electron Landau damping for finite $k_{\parallel}$ is strongly stabilizing.

The transport and heating associated with the nonlinear evolution of the lower hybrid drift instability, which can be described by an effective "anomolous" resistivity, have been calculated in a quasilinear analysis.[2] Particle simulations of the instability in both straight (θ-pinch) and reversed magnetic fields have also demonstrated that electron heating and transport can accompany the nonlinear development of the mode.[6,7]

Heating and transport are, by definition, irreversible processes and the subject of irreversibility must be addressed in discussing any transport or heating mechanism. In low temperature plasma collisions guarantee irreversibility on the macroscopic scale. In collisionless plasma, resonant wave particle interactions lead to irreversible exchanges of energy or momentum (and consequently transport). In the previous quasilinear investigation of heating by the lower hybrid drift mode, only perpendicularly propagating waves ($k_{\parallel} = 0$) were considered.[2] Ions, which behave as if they are completely unmagnetized (since $\omega \gg \Omega_i$), resonantly interact with the wave and exchange momentum and energy. The electrons, however, which are tightly bound to the magnetic field lines ($\omega \ll \Omega_e$) are nonresonant and therefore undergo no irreversible energy or momentum exchange (neglecting ∇B resonances). The quasilinear electron "heating" previously calculated simply results from the coherent sloshing of the electron distribution function in the lower hybrid waves and is completely reversible. In particular, for nonresonant particles, the heating rate is proportional to $\partial |\tilde{E}|^2/\partial t$, and the temperature increase scales as $|\tilde{E}|^2$, $\tilde{E}$ being the amplitude of the electric field perturbation. After an entire growth and damping cycle of the wave is completed, $|\tilde{E}|^2 \to 0$ and there is no net electron heating.

Although the quasilinear theory predicts that no irreversible electron heating can take place for $\underset{\sim}{k} \cdot \underset{\sim}{B} = 0$, computer simulations of the lower hybrid-drift-instability indicate that electron heating does actually occur.[6,7] These simulations are carried out in the two-space dimensions orthogonal to $\underset{\sim}{B}$ and consequently $k_{\parallel} = 0$. If this heating is a real physical effect and not a consequence of numerical errors, it must be associated with strong nonlinearities in the electron motion not property described by the quasilinear theory.

To develop an understanding of electron heating by the lower-hybrid-drift instability, we study the electron dynamics in a single large-amplitude, low

frequency ($\omega \ll \Omega_e$) wave propagating perpendicular to $\underset{\sim}{B}$,

$$E_y(y,t) = E_y^o(t) \cos(k_y y - \omega t) \quad , \qquad (1)$$

where the time dependence of $E_y^o(t)$ represents the growth or damping of the wave. The single mode approximation is a reasonable model of the simulations which were largely dominated by a single, coherent wave. Other physical effects including ∇B drifts, the two dimensionality of wave and the self-consistent evolution of the wave amplitude are neglected.

At small wave amplitude, the electron motion in this electric field is simply given by the usual $\underset{\sim}{E} \times \underset{\sim}{B}$ and polarization drifts and is accurately described by the quasilinear theory. Above a threshold given approximately by

$$k_y(cE_y/B\Omega_e) = k_y \Delta y \overset{\sim}{>} 1 \quad , \qquad (2)$$

the electron cyclotron motion is strongly modified and the electron motion becomes stochastic. The distance Δy in Eq. (2) is the y displacement of the electron due to the polarization drift. When this displacement is comparable to the wavelength of the electric field, the strong modification of the electron dynamics should not be too surprising. Above the threshold given in Eq. (2) substantial electron heating can occur.

The present investigation of electron dynamics is related to previous studies of stochastic ion motion in large amplitude waves. Smith and Kaufman studied the ion transition to stochastic motion in an obliquely propagating wave.[8] Stochastic particle motion in perpendicularly propagating waves has

also been investigated.[9]   However, the authors were primarily interested in

lower hybrid heating of ions and therefore, only considered cases where $\omega \gg \Omega_i$.

More recently, heating by a large amplitude standing wave has been studied.[10]

The present calculation is actually somewhat simpler than the previous in-

vestigations.   The existence of two disparate time scales Ω_e^{-1} and ω^{-1} allows

a straightforward analytic investigation of the electron motion and subsequently

to the threshold given in Eq. (2).

In Section II of this paper, the electron motion and transition to stoch-

asticity in a single wave is discussed.   In Section III, these results are

extended to an arbitrary number of waves in one-space dimension.   In contrast

with some turbulence theories based on the renormalization of particle orbits[11],

spatial diffusion is, strictly speaking, not possible in one-dimensional, low-

frequency turbulence.   In Section IV, the implications of these results for

the saturation and transport associated with the lower-hybrid-drift unstability

are discussed.   In Section V, the essential results and conclusions are summarized.

II. STOCHASTIC ELECTRON MOTION IN A SINGLE WAVE

The equations of motion for electrons in a plane wave propagating pendicular to a uniform magnetic field $\underset{\sim}{B} = B\hat{z}$ are simply

$$\ddot{y} = \Omega_e \dot{x} - eE_y/m_e \qquad (3)$$

$$\ddot{x} = -\Omega_e \dot{y} \qquad (4)$$

where $\Omega_e = eB/m_e c$ is the electron gyrofrequency, $E_y(y,t)$ is given in Eq. (1), and the dot denotes d/dt. Equation (4) can be integrated once and $\dot{x}$ can then be eliminated from Eq. (3) to obtain the single equation

$$\ddot{\theta} + \theta = \alpha \cos(\theta - \nu t + \phi) \qquad (5)$$

where $\theta = k_y y$, $\nu = \omega/\Omega_e$, $\alpha = -k_y eE_y^o/m\Omega_e^2$, time has been normalized to the gyrofrequency and ϕ is the initial phase. This equation has been studied previously in the limit $\nu \gg 1$.[9] We consider the opposite limit $\nu \ll 1$.

In the limit $\nu \to 0$, Eq. (5) can be integrated exactly to obtain the particle energy

$$H = \dot{\theta}^2/2 + \theta^2/2 - \alpha \sin(\theta + \phi) = \text{const.} \qquad (6)$$

The particle motion can be simply understood by plotting the constant H curves in the $\dot{\theta} - \theta$ phase plane as shown in Fig. 1a for $\alpha \ll 1$ and Fig. 1b for $\alpha \gg 1$. The electrons simply move along the constant H curves in this phase space. When $\alpha \ll 1$, these curves are essentially concentric circles weakly modified by the presence of the wave. The electric motion around these curves

on a time $t \stackrel{\sim}{\sim} 1$ corresponds to the usual electron Larmor motion. When $\alpha \gg 1$, the phase space structure becomes more complex with the formation of x and 0 points as can be seen in Fig. 1b. The electrons again circulate around the closed phase space curves on a time $t \stackrel{\sim}{\sim} 1$, except in narrow bands around the separations where the period becomes very long. In this limit the usual Larmor orbit is strongly modified by the presence of the wave. The islands shown in Fig. 1b correspond to regions where the perpendicular electric field is large enough to overcome the magnetic field and trap the electrons.

The location of the stationary points (x and 0 points) in the phase space of Fig. 1 can be calculated by solving $\partial H/\partial \theta = \partial H/\partial \dot{\theta} = 0$ or

$$\dot{\theta}_s = 0 \tag{7a}$$

$$\theta_s = \alpha \cos(\theta_s + \phi) \quad . \tag{7b}$$

The solutions to Eq. (7b) are shown graphically in Fig. 2. For $\alpha < 1$, there is a single 0 point as shown in Fig. 1a given by

$$\theta_s = \alpha \cos\phi \ll 1 \quad , \tag{8}$$

while for $\alpha > 1$, there are multiple x and 0 points increasing in number with α. For $\alpha \gg 1$, the solutions are approximately given by

$$\theta_s = -[\phi + (n + \frac{1}{2})\pi][1 + (-1)^n/\alpha] \quad , \tag{9}$$

where n is an integer and we have assumed $|\theta_s| \alpha \ll 1$. The outermost 0 point is given approximately by $\theta_s \stackrel{\sim}{\sim} \alpha$ (see Fig. 2).

The electron motion in the vicinity of the O-points of Fig. 1b can be investigated by expanding H in a Taylor series,

$$H \simeq \dot{\theta}^2/2 + \omega_b^2(\theta-\theta_s)^2/2 , \tag{10}$$

where $\omega_b^2 = \partial^2 H/\partial\theta^2 = [1+\alpha(1-\theta_s^2/\alpha^2)^{1/2}]^{1/2}$ is the bounce frequency of the electron in the potential well. For $|\theta_s| \ll \alpha$ (large islands in Fig. 1b), $\omega_b \simeq (1+\alpha)^{1/2} \simeq \alpha^{1/2}$, which corresponds to the usual bounce frequency $k_y(e\phi^o/m_e)^{1/2}$ of a trapped electron in the absence of the magnetic field. Note that since $\alpha>1$, the bounce frequency for these electrons is greater than the gyrofrequency. The bounce frequency of electrons in the smaller islands of Fig. 1b decreases monotonically with increasing $|\theta_s|$ until $\omega_b \gtrsim 1$ for the outermost islands.

When $\nu \neq 0$, the particle energy

$$H = \dot{\theta}^2/2 + \theta^2/2 - \alpha \sin(\theta - \nu t + \phi) , \tag{11}$$

the generalization of Eq. (6) for finite ν, is no longer a constant of the motion. However, in-so-far as $\nu \ll 1$, the energy is approximately conserved during the rapid gyro-motion discussed in Fig. 1 and this rapid motion is basically unchanged by ν, which simply enters Eq. (11) as a phase shift. On a longer time scale $\nu t \sim 1$, the particle energy change cannot be neglected. To simplify the discussion of the electron dynamics for $\nu \neq 0$, the two cases $\alpha \substack{<<\\>>} 1$ are considered separately.

A. <u>Small Amplitude Waves:</u> $\alpha \ll 1$

With $\nu \neq 0$ the constant H curves shown in Fig. 1a change on a time scale ν^{-1} and, in particular, the O-point oscillates periodically

$$\theta_s \simeq \alpha \cos(\phi - \nu t). \tag{12}$$

The particle energy H, which is no longer constant can be calculated directly,

$$\dot{H} = -\dot{\alpha} \sin(\theta - \nu t + \phi) + \nu\alpha \cos(\theta - \nu t + \phi) \quad . \tag{13}$$

where terms not proportional to $\dot{\alpha}$ or ν have been eliminated by invoking Eq. (5). To find the long time evolution of H, we average Eq. (13) over the fast cyclotron motion contained in $\theta(t)$,

$$\langle\dot{H}\rangle_t = -\dot{\alpha} \ \langle\sin(\theta - \nu t + \alpha)\rangle_t + \nu\alpha\langle\cos(\theta - \nu t + \phi)\rangle_t \quad . \tag{14}$$

For electrons near the 0-point of Fig. 1a, i.e., electrons with small Larmor radius, $\langle\sin(\theta - \nu t + \phi)\rangle_t \simeq \sin(\theta_s - \nu t + \phi)$ and

$$\langle\dot{H}\rangle_t \simeq -\dot{\alpha} \sin(\theta_s - \nu t + \phi) + \nu\alpha \cos(\theta_s - \nu t + \phi) \tag{15}$$
$$= d \ H(\theta_s, t)/dt \ ,$$

where $H(\theta_s, t)$ is the energy at the 0-point. Since the rate of change of the energy of the particle near the 0-point is the same as the energy of the 0-point, the particle must follow the 0-point. As the 0-point in Fig. 1a oscillates in θ, the particles simply follow along.

The average energy gain of the electrons over many oscillations ν^{-1} can be obtained by further averaging Eq. (15) over the time scale ν^{-1} under the assumption that $\dot{\alpha}/\alpha \ll \nu$. We find

$$\langle\langle\dot{H}\rangle\rangle_t \simeq -\dot{\alpha}\alpha/2 = -\frac{1}{4} d \ \alpha^2/dt \quad , \tag{16}$$

where higher order terms in α have been neglected and $<<>>_t$ represents the second time average over the ν^{-1} time scale. This change in the particle energy is simply the increase or decrease of the sloshing energy of the electrons in the wave as the wave amplitude changes and is entirely reversible.

The previous discussion of the small Larmor radius particles, which are localized near the 0-points can be easily generalized to arbitrary Larmor radius. Since the change in the constant H curves in Fig. 1a is much slower than the rapid cyclotron motion around the curves, the area within a particle orbit must be preserved, i.e.

$$J = \oint \dot{\theta} \, d\theta \tag{17}$$

is constant. In the previous calculation for electrons near the 0-point, the area within the orbit could only be preserved if the electron followed the 0-point. To demonstrate that no irreversible electron heating can occur for $\alpha < 1$ and arbitrary Larmor radius, we allow the wave amplitude α to increase to some maximum amplitude and then decrease to zero. Since the area within the particle orbit is the same in the initial and final states and the energy is a single valued function of the area, no net change in the particle energy can occur so all electron "heating" is reversible.

B. **Large Amplitude Wave:** $\alpha >> 1$

When $\nu \neq 0$, the islands shown in Fig. 1b for $\alpha > 1$ move toward positive θ with an approximate velocity $\dot{\theta} \approx \nu$, the phase velocity of the wave. More specifically, an island is formed at $\theta = -\alpha$ with zero amplitude. The x-point propagates with a velocity

$$\dot{\theta}_s^x \simeq \nu(1 + \alpha^{-1}) \qquad (18)$$

and the 0-point with a velocity

$$\dot{\theta}_s^0 \simeq \nu(1 - \alpha^{-1}) \quad . \qquad (19)$$

Thus, the island half width $\Delta\theta$ increases as the island propagates at a rate

$$\Delta\dot{\theta} \sim 2\nu/\alpha \quad . \qquad (20)$$

The island reaches maximum amplitude at $\theta = 0$ and then shrinks at the same rate and disappears at $\theta = \alpha$. The lifetime τ_s of a given island is therefore

$$\tau_s \simeq 2\alpha/\nu \quad . \qquad (21)$$

The motion of electrons which are far from the separatrices in Fig. 1b can be calculated in a fashion analagous to the weak field limit $\alpha < 1$. For example, an electron within an island in Fig. 1b must move toward positive θ to preserve the J invariant of its orbit. However, since the island shrinks and eventually disappears as it propagates toward $\theta = \alpha$, all electrons within a given island must eventually cross the separatrix of the island. As the electrons intercept the separatrix, the J invariant is broken since the period of the particle orbit on the separatrix is infinite and therefore no longer small compared with ν^{-1}. The detrapping or conversely the trapping of electrons is therefore an irreversible process. All electrons with energy $H < \alpha^2/2$ eventually participate in this trapping–detrapping process and we would therefore expect the electrons to eventually populate this entire phase space. Depending on the initial electron temperature, this strong wave–particle interaction produces substantial bulk electron heating. In unnormalized units, the

effective electron temperature becomes

$$T_e \approx m\, c^2 E_y^2/B^2 \quad , \tag{22}$$

i.e., the electron thermal velocity is simply cE_y/B.

Electron trapping by a large amplitude perpendicularly propagating wave has been observed previously in computer simulations of the electron beam cyclotron instability.[12] The qualitative features of the trapping-detrapping process for $\alpha \gg 1$ were observed. In these simulations, however, the wave frequency and electron cyclotron frequency were comparable ($\nu \sim 1$) and J was not a constant of the motion. We would expect, therefore, that electron trapping would be much less complete than in the case $\nu \ll 1$.

III. MULTIPLE WAVES

The invariance of J for the motion of electrons in a low frequency wave $\omega \ll \Omega_e$ was essential in deriving the stochasticity threshold in Eq. (1). As long as the low frequency assumption is satisfied, the previous calculation can be extended to include an arbitrary number of waves. The equation of motion for electrons in an arbitrary spectrum of one-dimensional, low-frequency waves is simply

$$\ddot{y} + y = -c \, E_y(y,t)/B\Omega_e^2$$

$$= -(c/B\Omega_e^2) \sum_k E_k \cos(ky - \nu_k t + \phi_k) \tag{23}$$

with an energy

$$H = \dot{y}^2/2 + y^2/2 - (c/B\Omega_e^2) \sum_k E_k \sin(ky - \nu_k t + \phi_k)/k \quad . \tag{24}$$

The electron motion can again only become stochastic once multiple stationary points are formed, which requires

$$\partial E_y/\partial y > \Omega_e B/c \quad . \tag{25}$$

When this threshold is exceeded locally, electron heating can occur. In most physical systems of interest, precise wave phase information is not available and a threshold based on averaged stochastical properties of the wave turbulence is desireable. If the phases ϕ_k of the individual waves are random, we simply square Eq. (25) and average over the random phases to obtain the stochasticity condition

$$\sum_{k} |cE_k/B|^2 \, k^2/\Omega_e^2 > 1 \quad .$$

(26)

Particle motion in random-phased, perpendicularly propagating waves has been discussed by a number of authors in connection with turbulence theories based on the renormalization of particle propagators. Dum and Dupree investigated particle motion in a general spectrum of low frequency fluctuations.[11] In their formalism, electrons can undergo spatial diffusion in a one-dimensional spectrum of waves once the following threshold is exceeded,

$$\sum_{k} |cE_k/B|^2 \, k^4 \rho_e^2/\omega^2 > 1 \quad ,$$

(27)

where $\rho_e = v_e/\Omega$ is the electron Larmor radius. In contrast, the present calculation demonstrates that the spatial excursion of electrons is always bounded since the constant H curves are always closed. Spatial and velocity diffusion are only possible in the limited sense that the electron position and velocity can scatter over a bounded region of phase space [for example, $H < \alpha^2$ in Fig. 1b] and only when the threshold given in Eq. (26) is exceeded. A more detailed discussion of the absence of spatial diffusion in this one-dimensional model is presented in Appendix A.

IV. <u>APPLICATION TO THE LOWER HYBRID DRIFT INSTABILITY</u>

The basic properties of the lower-hybrid-drift instability have been
briefly mentioned in the Introduction and have been extensively discussed in
the literature.[1-3] The instability essentially causes the plasma density
profile to become fluted perpendicular to $\underset{\sim}{B}$. Below the thresholds given
in Eq. (2) in the case of a single wave and Eq. (24) for the case of many
waves, the electrons simply undergo coherent oscillations in the wave and the
lower-hybrid-drift wave cannot irreversibly exchange energy or momentum with
the electrons. Thus, if the instability saturates before this threshold is
exceeded, the lower-hybrid-drift instability cannot cause anomalous diffusion
of an inhomogeneous plasma. In this limit, the plasma essentially evolves
to a complicated fluted state but the mechanism by which this fluted state
can evolve to a diffuse profile must involve new physics not yet incorporated
into the present model.

The distinction between the evolution of an inhomogeneous plasma to a
fluted state and the evolution to a more diffuse profile has not been
adequately addressed within the literature, possibly because it has been
assumed that once the flutes develop, the evolution to a broader
smooth profile was an inevitable process. In computer simulations of the
lower-hybrid-drift instability, for example, the formation of these flutes has
been observed. The density profile is then calculated by averaging over
these flutes. This averaging process can produce an apparent broadening of
the plasma profile even though no diffusion has actually occurred. To
illustrate this point, we consider a periodic displacement of the density
profile

$$n(x,y) = n_o \left[x + \overset{\sim}{\Delta} x(y) \right] . \qquad (28)$$

where $x(v)$ is the displacement. Clearly, no diffusion has taken place since for a given v, the plasma profile is unchanged. Yet when $n(x,v)$ is averaged over v, we find

$$\langle n \rangle \equiv \langle n(x,y) \rangle_y = n_0(x) + \langle \Delta x^2 \rangle_y \, \partial^2 n_0 / \partial x^2 . \tag{29}$$

The profile has effectively diffused as shown in Fig. 3. This fake "diffusion" is analogous to the electron "heating" associated with the coherent sloshing of electrons in the wave. In computer simulations of this instability, very little real diffusion is observed in the weak drift regime $v_{di} < v_i$ while in the stronger drift regime $v_{di} \gg v_i$ real diffusion is observed.[7] We now consider under what conditions the thresholds in Eqs. (2) and (26) can be exceeded, allowing transport to take place.

Three basic saturation mechanisms for the lower-hybrid-drift instability have been discussed: (1) trapping or flattening of the ion velocity distribution function;[6,13] (2) depletion of the free energy available to drive the instability;[4,6,13] and (3) electron resonance broadening.[14] The lower-hybrid-drift instability is basically a negative energy wave driven by ion Landau damping. Flattening of the ion distribution either by quasilinear relaxation or trapping can therefore lead to saturation by quenching the ion Landau damping.

The energy source of the lower-hybrid-drift mode is the drift energy produced by the local gradients, $nmv_{di}^2/2$. It was previously predicted that the wave energy

$$W_E = \omega(\partial\varepsilon/\partial\omega)(E_y^2/8\pi)$$

$$= 2(1 + \omega_{pe}^2/\Omega_e^2)(E_y^2/8\pi) \tag{30}$$

could not exceed the particle drift energy[4] or that the electric field fluctuation must satisfy

$$(cE_y/B)^2 < v_{di}^2 / [2(1 + \Omega_e^2/\omega_{pe}^2)] \quad . \tag{31}$$

In a finite beta system, of course, the drift energy and magnetic energy are linked so that the magnetic energy also changes as the local gradients change.[15] In a straight θ-pinch, the change in the magnetic energy ΔW_B as the gradient relaxes is approximately (see Appendix B)

$$\Delta W_B = n(T_e + T_i) \, g(\beta) \tag{32a}$$

with

$$g(\beta) = [(1+\beta)^{1/2} - 1] / [(1+\beta)^{1/2} + 1], \tag{32b}$$

where $\beta = 8\pi n(T_e + T_i)B^2$ is a representative value of the local plasma beta. This magnetic free energy exceeds the drift energy as long as $v_{di}/v_i < (m_i/m_e)^{1/2}$ so the wave energy bound becomes

$$(cE_y/B)^2 < v_{es}^2 \, g(\beta) / [1 + \Omega_e^2/\omega_{pe}^2] \quad , \tag{33}$$

where $v_{es}^2 = (T_e + T_i)/m_e$. In a system where the particle drifts support a reversed magnetic field, such as a reversed field θ-pinch, the gradients cannot be relaxed without dissipating all the magnetic energy in the system, the free energy available to drive the instability is effectively infinite and there is no wave energy bound.[16]

Resonance broadening has also been proposed as a saturation mechanism for the lower-hybrid-drift instability.[14] Once the fluctuating electric fields exceed a critical amplitude, the electrons, which are initially nonresonant, can effectively resonantly interact with the waves. The resulting "Landau" damping of the wave energy stabilizes the wave spectrum. The threshold at which this transition takes place is, of course, the subject of this paper and is given by either Eq. (2) or Eq. (26) in the case of single or multiple waves, respectively. These thresholds are substantially higher than those

predicted on the basis of resonance broadening theory [Eq. (27)].

Above the stochasticity threshold, strong electron heating takes place, thus dissipating the wave energy and stabilizing the lower hybrid drift wave. If ion trapping or depletion of the free energy do not occur first, the lower-hybrid-drift instability will saturate at an amplitude given by either Eq. (2) or Eq. (26). In the previous application of the resonance broadening theory to the lower-hybrid-drift instability, substantially lower thresholds were predicted when electron ∇B drifts were included.[14] The question of the validity of the resonance broadening theory in the presence of the ∇B drifts cannot be addressed on the basis of the present calculation. The reduction of the stochasticity threshold by the ∇B drift, however, seems physically reasonable, and the inclusion of these effects would be an important extension of the present work.

We now consider under what conditions saturation of the lower-hybrid-drift instability can occur by stochastic electron heating. The growth rate of the lower-hybrid-drift instability peaks in the range $k\rho_{es} \simeq 1-2$, where $\rho_{es}^2 \simeq v_{es}^2/\Omega_e^2$, so the electron stochasticity threshold in Eq. (2) becomes

$$e\phi/T_i \sim (k\rho_{es})^{-2} \simeq .25 - 1 \quad . \tag{34}$$

In the weak drift limit $v_{di}/v_i \ll 1$, the phase velocity of the wave is $v_{ph} \sim v_{di} \ll v_i$. The saturation of the instability can occur by flattening the ion velocity distribution or ion trapping at an amplitude

$$e\phi \simeq m_i v_{ph}^2/2 = m_i v_{di}^2/2 \ll T_i \tag{35}$$

even in the absence of the wave energy bound.[13] This amplitude is below the

threshold for electron stochasticity given in Eq. (34) so no electron diffusion is possible in the weak drift regime. In the strong drift regime $v_{di} \sim v_i$, ion trapping occurs when $e\phi \sim m_i v_{ph}^2/2 \stackrel{\sim}{>} m_i v_i^2/2$ or[6]

$$e\phi/T_i > 1 \qquad (36)$$

so the electron stochasticity and ion trapping conditions are comparable. In the case of a reversed magnetic field in the strong drift regime both ion trapping and electron stochasticity should cause saturation of the instability and strong electron heating and diffusion can occur. For $k_y \rho_{es} < 1$, the wave energy bound in Eq. (33) for the straight pinch can be rewritten as

$$e\phi/T_i < g(\hat{r}) \quad . \qquad (37)$$

In a high β configuration this bound is comparable to the ion trapping and electron stochasticity conditions so that diffusion and heating will occur. In a low β configuration the energy bound is smaller than either of these conditions and no diffusion is possible.

Two-dimensional particle simulations of the lower-hybrid-drift instability have been carried out in both straight and reversed magnetic fields.[6,7] These runs were carried out for relatively strong drift $v_{di}/v_i \sim 1$ 10 with relatively large $\beta \sim 0.25-1.0$ and artificial mass ratios. As a consequence, the wave energy bounds in Eqs. (31) and (37), the ion trapping threshold in Eq. (36) and the electron stochasticity threshold in Eq. (34) are all comparable even for the straight pinch. Electron heating should therefore be expected, especially in the strong drift regime $v_{di}/v_i \gg 1$. In the case of $v_{di}/v_i \sim 1$ fluting of the density profile is observed in the simulations but the mode saturates with very little actual broadening of the profile.[7] In the strong drift regime both strong electron heating and diffusion are observed, as expected.

V. SUMMARY AND CONCLUSIONS

Electron motion in a low-frequency ($\omega \ll \omega_e$) wave(s) propagating per-
pendicular to a uniform magnetic field is studied. Both monochromatic and
broadband electric field spectra have been considered although the investigation
is strictly limited to one-dimensional spectra. Below a threshold amplitude
given by

$$\alpha = k_y \ c \ E_y/B\Omega_e \simeq 1 \tag{37}$$

for the case of a monochromatic wave and the corresponding generalization

$$\sum_k |k \ cE_k \ /B\Omega_e|^2 \simeq 1 \tag{38}$$

for a broadband spectrum of waves, electron heating and momentum transfer
are strictly reversible. Above these thresholds, the Larmor motion of an
electron in a uniform magnetic field is strongly modified and trapping of the
electrons by the wave can occur. The electrons remain trapped for a time τ_{tr}
given by

$$\tau_{tr} \simeq k_y cE_y/B\omega\Omega_e = \alpha/\omega \gg \Omega_e^{-1}, \ \omega^{-1} \tag{39}$$

The process of trapping and detrapping allows an irreversible exchange of energy
between the electrons and the wave and, in particular, causes bulk "heating"
of electrons to a mean velocity

$$v_\perp \sim v_E = cE_y/B \ . \tag{40}$$

This trapping-detrapping phenomena has been previously observed in computer simulations of the electron beam cyclotron instability, although the trapping is much less complete in this limit because $\omega \sim \Omega_e$.[12]

The implications of these results for the nonlinear evolution of the lower-hybrid-drift instability and associated transport have been explored. The growth rate of the lower-hybrid-drift instability peaks for $k\rho_{es} = k(T_i/m_e)^{1/2}/\Omega_e \simeq 1-2$ so the threshold in Eq. (37) becomes

$$e\phi/T_i \simeq .25 - 1 \quad . \tag{41}$$

Below this threshold no irreversible electron heating or momentum transfer is possible and the lower-hybrid-drift instability cannot cause diffusion of electrons in an inhomogeneous plasma. The apparent diffusion which is found from quasilinear theory in this limit corresponds to the formation of flutes or ripples in the plasma profile — not to the evolution to a more diffuse profile. In the weak drift regime $v_{di} < v_i$, the lower-hybrid-drift instability saturates below the threshold given in Eq. (41) by trapping ions or depleting the source of free energy,[13] and transport by the lower hybrid drift instability is not possible (at least within the limitations of the present model).

In the strong drift regime $v_{di} > v_i$, the lower hybrid drift instability grows until the threshold in Eq. (41) is exceeded. The rapid onset of strong electron heating above this threshold prevents further amplifications of the wave and thus saturation of the instability occurs for $e\phi/T_i \gtrsim 1$. Electron heating, transport, and magnetic energy dissipation accompany the saturation of the mode in this limit[16] and have been observed in recent computer simulations of the lower-hybrod-drift instability in a reversed magnetic field.[7]

It should be emphasized that these conclusions are strictly based on the present limited model: (1) a one-dimensional wave spectrum; (2) $k_{\parallel} = \underset{\sim}{k} \cdot \underset{\sim}{B} / |B| = 0$; and (3) a uniform magnetic field. The relaxation of these assumptions should lead to a reduction of the threshold given in Eq. (31) and allow the lower-hybrid-drift instability to cause anomalous transport in the weak drift regimes.

APPENDIX A

We now consider in more detail, the electron dynamics in a one-dimensional spectrum of low frequency ($\omega \ll \Omega_e$) waves. The electron equation of motion is given in Eq. (23),

$$\ddot{y} + y = -cE_y(y,t)/B\Omega_e^2 \equiv -\varepsilon(y,t) \ . \tag{A1}$$

We have shown that the electron motion is bounded and y therefore remains finite for all time. For simplicity, we limit our investigation to the case where the stochasticity threshold in Eq. (26) is not exceeded and the electron Larmor radius is small compared to the wavelength of the fluctuations. In this case, $\varepsilon(y,t)$ can be expanded around $y \approx 0$,

$$\ddot{y} + y(1 + \partial\varepsilon/\partial y) = -\varepsilon(0,t) \ . \tag{A2}$$

The electric field fluctuations cause a frequency shift of the electron gyro-motion $\delta\Omega(t) = (\partial\varepsilon(y,t)/\partial y)\big|_{y=0}$. The solution of Eq. (A2) is

$$y(t) \simeq -\varepsilon(t) + \rho_e \cos(t + \phi + \delta\phi), \tag{A3}$$

where ρ_e is the electron Larmor radius, ϕ is the initial phase angle of the electron in its gyromotion and

$$\delta\phi(t) = \int_0^t d\tau \ \delta\Omega(\tau) \ , \tag{A4}$$

is the phase shift induced by the fluctuating electric field. Averaging y(t) over an ensemble of fluctuations,

$$\langle y(t) \rangle = \rho_e \langle \cos(t + \phi + \delta\phi) \rangle$$

$$\quad (A5)$$

$$= \rho_e \cos(t + \phi) \exp[-\Phi(t)/2] \ ,$$

where

$$\Phi(t) = \int d\tau_1 d\tau_2 \langle \delta\Omega(\tau_1)\delta\Omega(\tau_2) \rangle \ , \qquad (A6)$$

$\langle \rangle$ denotes an average over the ensemble and the cumulant expansion has been used to evaluate $\langle \exp(i\delta\phi) \rangle = \exp(-\Phi/2)$.[17] The electron diffusion can similarly be calculated,

$$\langle \delta y^2 \rangle = \langle (y - \langle y \rangle)^2 \rangle = \langle \varepsilon^2 \rangle + (\rho_e^2/2)[1 - \exp(-\Phi)]. \qquad (A7)$$

If the electric field fluctuations have a finite correlation time τ_c, then for $t > \tau_c$,

$$\langle \delta y^2 \rangle = \langle \varepsilon^2 \rangle + (\rho_e^2/2)[1 - \exp(-\dot{\Phi}t)] \qquad (A8)$$

where

$$\dot{\Phi} = (2\pi)^{-1} \int dk \ d\omega \ \delta(\omega) \ |\delta\Omega_{k\omega}|^2 \ . \qquad (A9)$$

The first term in Eq. (A8) corresponds to the mean excursion of the electron associated with its polarization drift. The second term arised because of the frequency shift of the electron Larmor motion. The phase of the electrons along their orbits becomes uncertain and is reflected in an uncertainty in their position. Over short times this appears as a diffusion

$$\langle \delta y^2 \rangle \approx \rho_e^2 \ \dot{\Phi} \ t/2 \qquad (A10)$$

of the particle position [compare with Eq. (7) in Ref. 14 in the long wavelength

limit]. However, over longer times $\dot{\phi}t > 1$, the maximum uncertainty in the particle position is $\rho_e^2/2$, i.e., the phase angle of the electron in its Larmor orbit is completely unknown. Thus, spatial diffusion is possible below the threshold given in Eq. (26) for t_c finite but is limited to the electron Larmor radius. This result is consistent with the previous discussion of the preservation of the J invariant in Fig. 1a. The phase of the electron along the curves shown in Fig. 1 can become uncertain but the area within the curve is still preserved and thus diffusion is strictly limited.

It should also be noted that even the limited diffusion described by Eq. (A8) is produced only by the zero frequency component of the wave spectrum [see Eq. (A9)]. The frequency shift of the $\omega \neq 0$ waves is periodic and causes no net phase shift of the electrons in their Larmor motion. In a spectrum of high frequency waves no diffusion occurs unless the threshold in Eq. (26) is exceeded. The "bootstrap" diffusion calculated by Dum-Dupree when the threshold in Eq. (27) is exceeded does not take place because the excursion of electrons in the fluctuating electric fields is strictly bounded (there is no orbit secularity).

APPENDIX B

The lower hybrid drift instability is driven by the drift energy of the electrons, $n\, m_e\, v_d^2/2$. However, in a finite β plasma the magnetic field and the plasma currents are linked so the plasma currents can not be relaxed without changing the magnetic energy. When the plasma currents support a reversed magnetic field, the plasma current can not be dissipated without dissipating all the magnetic energy in the system so there is effectively no energy bound for the lower hybrid drift instability.[16] We now consider the change in magnetic energy as the plasma profile broadens in the straight θ pinch.

For simplicity, the plasma profile is modeled by the simple step shown in Fig. 4 (the profile is taken to be symmetric around x=0). An initial plasma of density n_i, temperature T_i and in a magnetic field B_1^i is supported by an external magnetic field B_o. The initial plasma width L_1^i is allowed to increase. Conducting boundaries at $X=L_o$ prevent flux from entering or leaving the system so the total flux

$$A = B_1^i L_1^i + B_o(L_o - L_1^i) \tag{B1}$$

is constant. The total number density $N = n^i L_1^i$ is also conserved. The change in the particle drift energy is ignored since this can only increase the free energy available to drive the lower hybrid drift instability.

Local pressure balance

$$B_o^2/8\pi = B_1^2/8\pi + nT \tag{B2}$$

will also be maintained during the evolution of the profile. Flux and particle conservation are invoked to eliminate B_1 and n from (B2) to obtain an expression for T,

$$T/T^i = [2B_o L_1 - L_1^i(B_o - B_1^i)]/[L_1(B_o + B_1^i)] > 1 \ . \tag{B3}$$

When $L_1 \gg L_1^i$, $T/T^i = |B_o/(B_o + B_1^i)$ or the increase in temperature $\Delta T = T - T^i$ is given by

$$\Delta T = T - T^i = T^i[(1+\beta^i)^{1/2}-1]/[(1+\beta^i)^{1/2}+1] \tag{B4}$$

where $\beta^i = 8\pi n^i T^i / B_1^{i^2}$ is the initial plasma beta. In a low β system the temperature increase is given by

$$\Delta T^i \simeq T^i \beta^i/2 \ll T^i . \tag{B5}$$

In a high β system, however, the plasma heating can be substantial with

$$\Delta T^i \simeq T_i .$$

This increase in the plasma thermal energy is matched by a corresponding reduction in the magnetic energy, i.e., as the sheath broadens, the system evolves to a lower magnetic energy state. This energy must be included in the free energy available to drive the lower hybrid drift mode since the plasma currents can not be relaxed until all of the magnetic energy has been dissipated. Although the expression for ΔT in Eq. (B4) was derived for the rather simplified step model in Fig. 4, the qualitative scaling with β is valid for a more general profile and will be discussed in a subsequent publication.[15]

ACKNOWLEDGEMENTS

REFERENCES

1. N. A. Krall and P. C. Liewer, Phys. Rev. A4, 2094 (1971).

2. R. C. Davidson and N. T. Gladd, Phys. Fluids 18, 1327 (1975).

3. R. C. Davidson, N. T. Gladd, C. S. Wu and J. D. Huba, Phys. Fluids 20, 301 (1977).

4. P. C. Liewer and R. C. Davidson, Nuc. Fusion 17, 85 (1977).

5. J. D. Huba, N. T. Gladd and K. Papadopoulos, Geophys. Res. Lett. 4, 125 (1977).

6. D. Winske and P. C. Liewer, Phys. Fluids 21, 1017 (1978).

7. D. Winske, private communication.

8. G. R. Smith and A. N. Kaufman, Phys. Rev. Lett. 34, 1613 (1975).

9. C. F. F. Karney and A. Bers, Phys. Rev. Lett. 39, 550 (1977); C. F. F. Karney, Phys. Fluids 21, 1584 (1978).

10. J. Y. Hsu, K. Matsuda, M. S. Chu and T. H. Jensen, Phys. Rev. Lett. 43 203 (1979).

11. C. T. Dum and T. H. Dupree, Phys. Fluids 13, 2064 (1970).

12. D. W. Forsland, R. L. Morse and C. W. Nielson, Phys. Rev. Lett. 27, 1424 (1971); Phys. Fluids 15, 1303 (1972).

13. R. C. Davidson, Phys. Fluids 21, 1017 (1978).

14. J. D. Huba and K. Papadopoulos, Phys. Fluids 21, 121 (1978).

15. J. D. Huba, J. F. Drake and N. T. Gladd (to be published).

16. J. D. Huba, J. F. Drake and N. T. Gladd, Phys. Fluids 23, XXX (1980).

17. J. Weinstock, Phys. Fluids 12, 1045 (1969).

FIGURE CAPTIONS

Fig. 1.   Constant H curves are shown in the θ-$\dot{\theta}$ phase plane for $\alpha = .5$,

$\phi = 0$ in (a) and $\alpha = 8\pi$, $\phi = \pi/2$ in (b).

Fig. 2.   The positions of the stationary points $\theta_s = \alpha \cos(\theta_s + \phi)$ are shown

graphically for the parameters of Fig. 1b.

Fig. 3.   The pseudo-diffusion $\langle n_o[x+\Delta x(y)]\rangle_y \simeq n_o(x) + (1/2)n_o''\langle\Delta x^2\rangle_y$ which

results from the periodic displacement $\Delta x(y)$ of an initial

plasma profile $n_o(x)$ is shown.   The bracket $\langle\rangle_y$ denotes a spatial

average over y.

Fig. 4.   The θ-pinch profile is modeled by a simple step in the magnetic

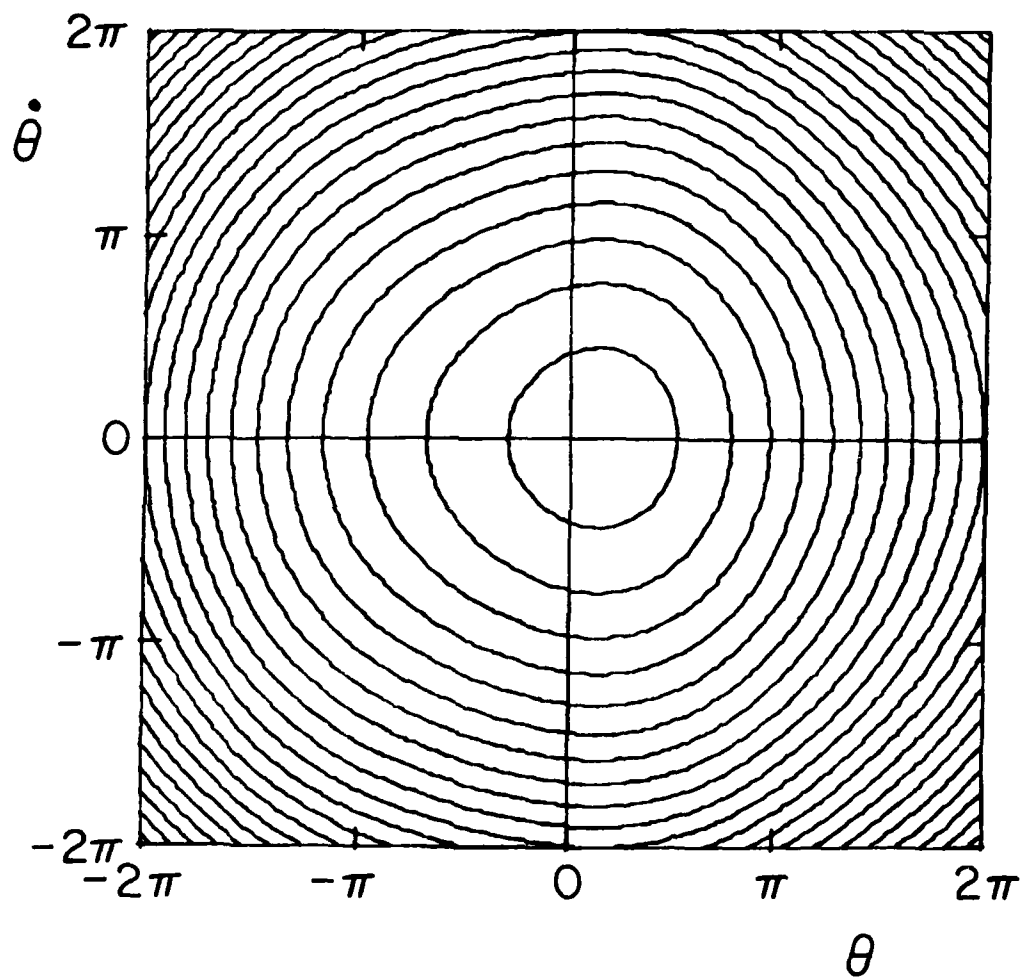field profile.   The profile is symmetric around x=0.
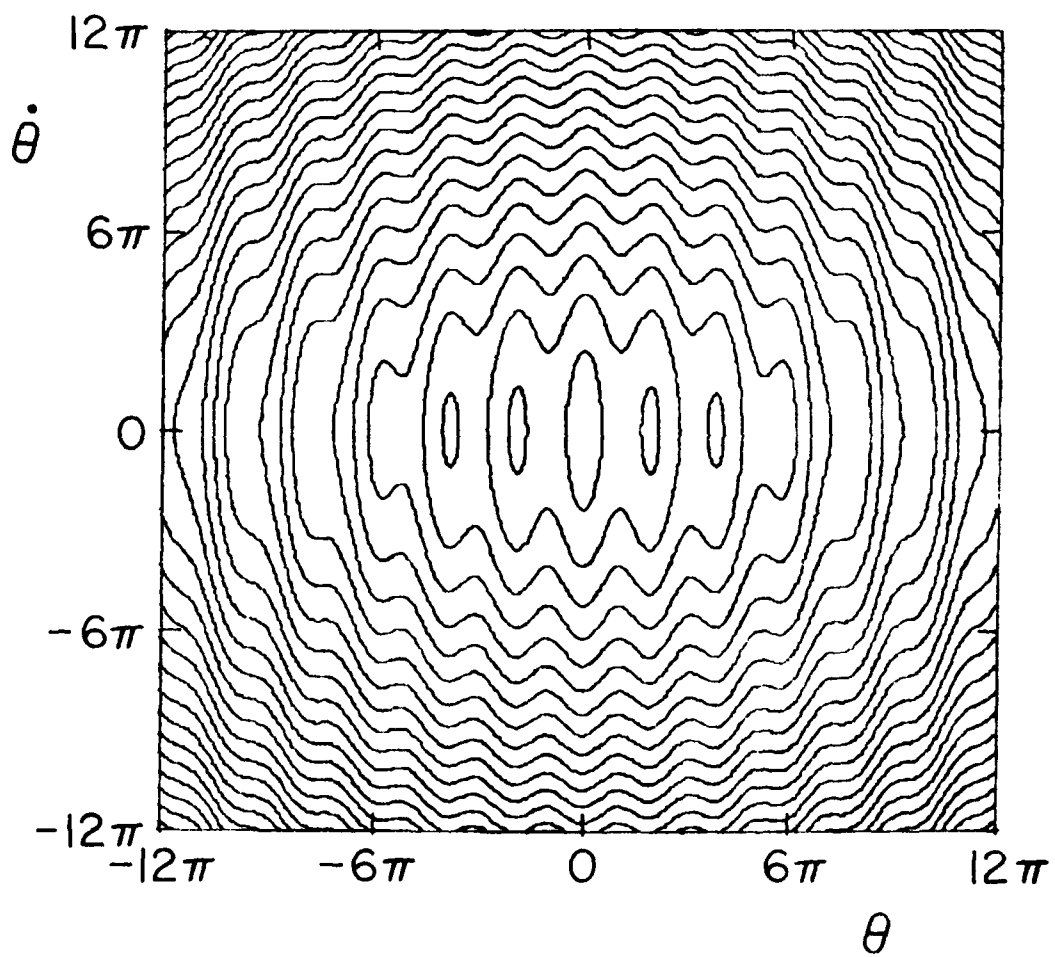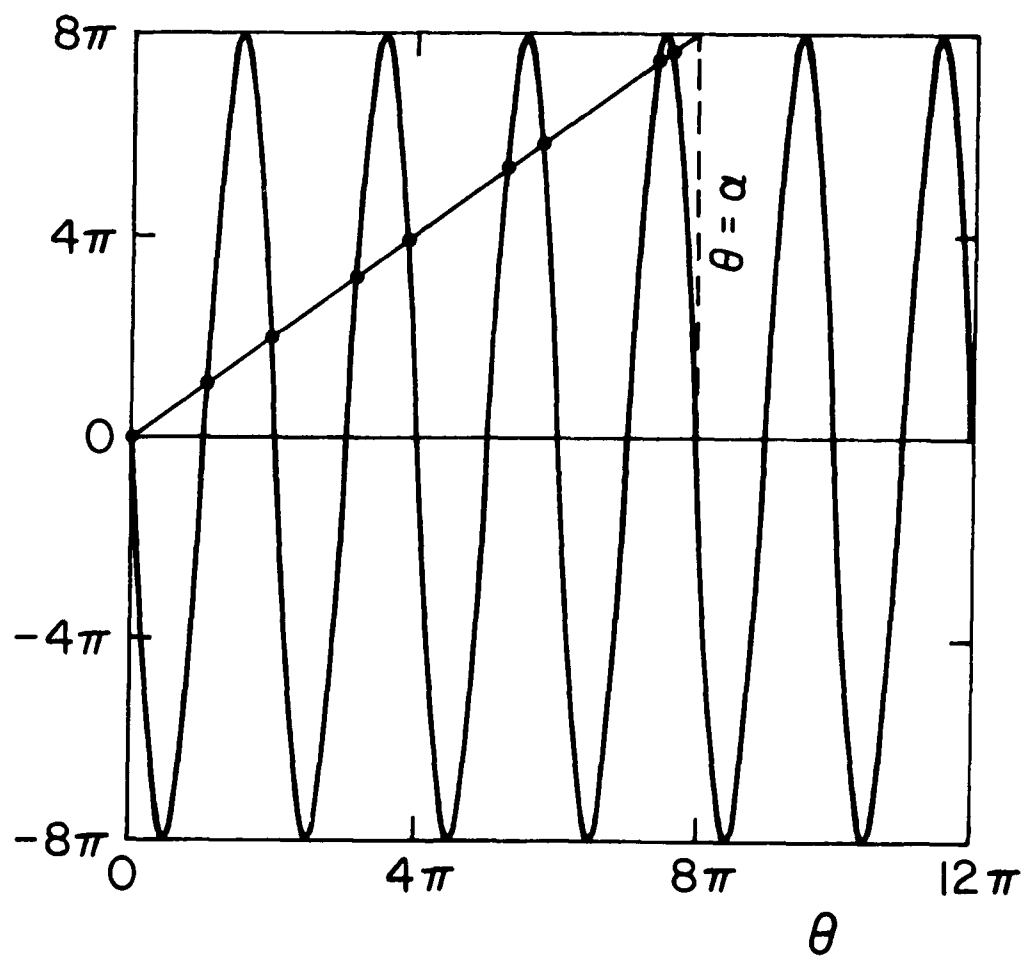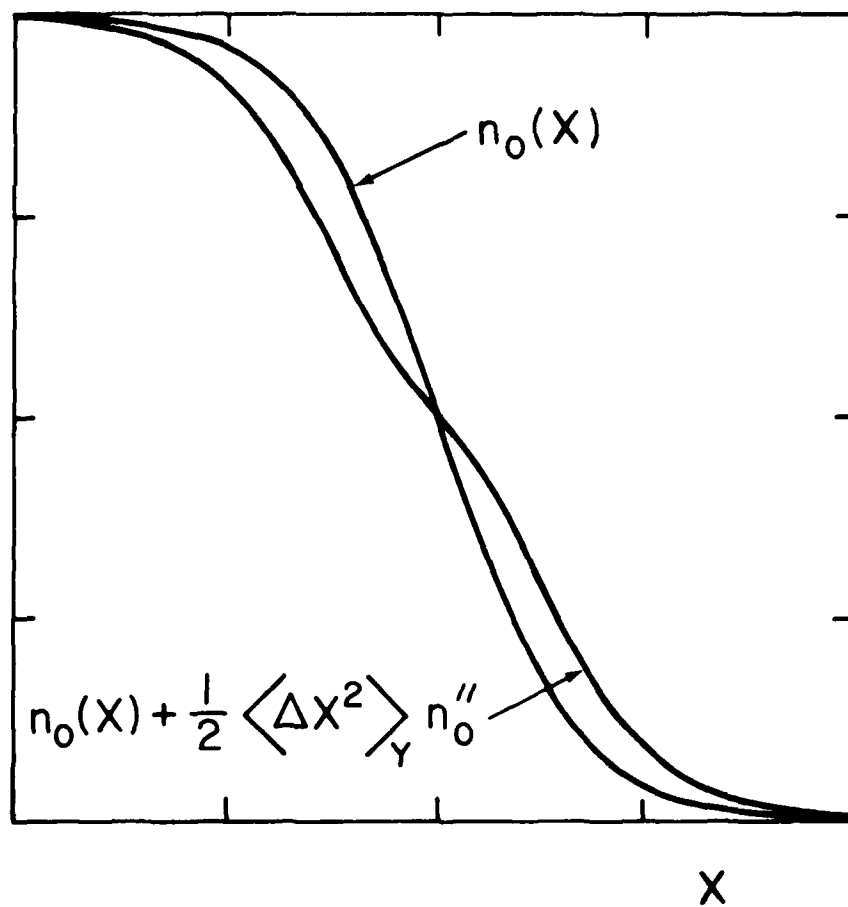
Figure 1a

Figure 1b

Figure 2

$$n_0(X)$$

$$n_0(X) + \frac{1}{2} \left\langle \Delta X^2 \right\rangle_Y n_0''$$

X

Figure 3

Figure 4